



# A Periodic Heating into Different Layers of a Semi-Infinite Solid

Shalom Sadik<sup>1</sup>

Received: 7 August 2020 / Accepted: 20 January 2021 / Published online: 4 February 2021  
© The Institution of Engineers (India) 2021

**Abstract** This paper deals with a periodic heating into different layers of a semi-infinite solid in order to examine the thermal parameters influence of the different layers on the development of the temperature oscillations. This influence is introduced by a physical model that shows the temperature evolution in every location into the solid layers as a function of time. It was shown that the structure with the larger thermal conductivity in the semi-infinite layer has larger absolute gradient of temperature on the external surface (the system left surface). Received at certain times temperature distributions with extreme, maximum or minimum temperatures values. These values actually represent adiabatic surfaces at the relevant times, meaning that heat transfer, entry or exit occurs in the limited volume between the constraint surface and those adiabatic surfaces. These temperature distributions also show receiving of identical, positive or negative values along all the medium depth. At the start time of the time period and at the half time of the time period, linear temperatures distributions are obtained. These times can be seen as weakening times in terms of supporting the transient heat transfer. The temperature distribution in the structure of a wall made up of real building materials shows that the wall is a retainer for temperature fluctuations and not just is a basic resistance to heat transfer.

**Keywords** Temperature · Oscillations · Distribution · Transient · Steady state

## Introduction

Stokes second problem described by Schlichting [1] was and still is a basis of many research directions not only in the specific area of the problem. The problem describes a semi-infinite flow field which is disturbed by an oscillating plate  $u(0, t) = U_0 \cos(\omega t)$  where  $u(0, t)$  designate the plate velocity or the bottom layer velocity of the fluid as a function of time,  $U_0$  is the plate velocity amplitude and  $\omega$  is the plate frequency. The essence of the problem is that the fluctuations in the fluid can be seen as a kind of steady-state condition despite the fluid velocity values do change over time but get the same values in equal time periods. Stokes problem has been extended to the realm of non-steady or transient state, an example of such work being that of Panton [2]. Nazar et al. [3] and Asghar et al. [4] expanded the Stokes problem to the transient realm for second grade fluids. The following are more examples of expanding the Stokes problem. Srinivasan and Rajagopal [5] and Prusa [6] expanded the Stokes problems to pressure dependent viscosities. Dutta and Beskok [7] introduced an analytical solution of time periodic electroosmotic flows, it was shown that for some of the cases investigated the flow is analogies to Stokes second problem.

Khaled [8] investigated the influence of combined periodic heat flux and convective boundary condition on heat conduction through a semi-infinite and finite media. It was found that the temperature fluctuations in each medium decreased as the Bio number was increased. Ahmadi et al. [9] presented an analytical solution of transient heat flux condition on skin tissue as a finite domain, it was shown that by penetrating along the skin depth the temperature amplitude response decreases significantly. Some more examples of physical models developed for describing transient heat conduction in a slab or through more than

✉ Shalom Sadik  
shaloms@braude.ac.il

<sup>1</sup> Mechanical Engineering, ORT Braude College of Engineering, Karmiel, Israel

one material layer are the works of Sadat [10], Norouzi et al. [11] and that of Shiah and Shi [12].

Kundu [13] examined five boundary conditions in order to determine the temperature response in a biological tissue under Fourier and non-Fourier heat conduction. The paper ultimate goal was to improve thermal therapy for killing cancerous cells without side effects. The representing equation was built according to the bioheat transfer equation for Fourier and non-Fourier heat conduction. The thermal response of the skin tissue was solved by the separation of variables method. It was found that the higher temperature response was received by isothermal heating for the non-Fourier heat conduction in the tissue. This may be selected as a design condition for effective heating. Kundu and Lee [14] used a semi-analytical method in order to investigate the thermal performance of fin and tube heat exchangers with orthotropic fin material and wet surfaces. It was found that the fin efficiency of orthotropic materials was always lower than that of the isotropic material and the efficiency of wet fins decreased with increasing the relative humidity of the air for a constant base and ambient temperatures. Kundu and Lee [15] determined analytically the temperature distribution for 2D heat conduction in a fin. The 2D physical model was solved by using the separation of variable method. It was found that the 2D heat conduction in a fin is primarily dependent upon the geometry of the fin and base temperature.

There are several technology areas that may require a study of heat transfer oscillations on a semi-infinite board, for example, a material processing using laser beams and microwave heating. The present work is actually implementing the second Stokes problem for a semi-infinite heat transfer where the oscillating velocity disturbance is replaced by the oscillating temperature. In addition, within the semi-infinite medium, a material layer of a finite thickness and different thermal conductivity was inserted. The temperature penetration or heat transfer at this stratified medium is discussed in this work.

## Mathematical Formulation and Solution (The Physical Model)

The development of the physical model described here is fully inspired by the solution of the physical model of Stokes' second problem. Stokes' second problem was presented by Schlichting [1] based on the original article [16]. Stokes' second problem describes the effect of forced oscillations on the space of an incompressible fluid in a semi-infinite medium. Although there are fluctuations in the problem and it is time dependent, in fact this condition is a condition that is ostensibly a steady-state condition and therefore there are actually no initial condition but only

boundary conditions. Because the problem describes one representative frequency that is forced into the whole space of the problem and because the state is ostensibly a steady state despite the oscillations, the conventional move of searching for additional self-values and subsequent use of the orthogonal connection is not obligatory (Fig. 1).

The drive of the temperature oscillations is expressed by the following connection:

$$T(0, t) = T_i + \Delta T \cos(\omega t) \quad (1)$$

where  $\omega$  is the oscillation frequency and  $\Delta T$  is the disturbance amplitude. Without any disturbance or while  $\Delta T = 0$  the temperature in every point into the materials layers is equal to  $T_i$ . As can be seen, the maximum temperature on the surface is received when  $t = 0$  and is equal to  $T_i + \Delta T$ . Equation (1) can be written as:

$$T(0, t) - T_i = \Delta T \cos(\omega t) \quad (2)$$

or as:

$$T(0, t) = T_i + (T_0 - T_i) \cos(\omega t) \quad (3)$$

where  $T_0$  is the maximum temperature on the surface or actually is the maximum temperature that can be received in every point into the materials layers and is equal to  $T_i + \Delta T$ .

It is signified that:

$$\theta = T - T_i \quad (4)$$

where  $T$  denotes the temperature value in every point into the materials layers. It can be concluded that  $\partial T / \partial x$  is equal to  $\partial \theta / \partial x$ , that  $\partial^2 T / \partial x^2$  is equal to  $\partial^2 \theta / \partial x^2$  and that  $\partial T / \partial t$  is equal to  $\partial \theta / \partial t$ .

It can be written:

$$\theta(0, t) = T(0, t) - T_i \quad (5)$$

If the significance of  $\Delta T$  is that:

$$\Delta T = T_0 - T_i \quad (6)$$

The following notation can be written:

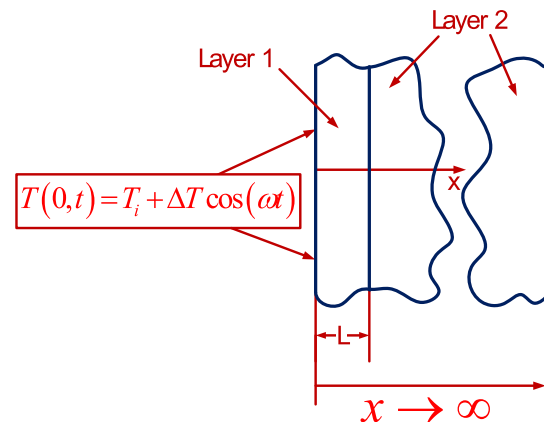


Fig. 1 The problem structure

$$\theta_0 = T_0 - T_i \tag{7}$$

and:

$$\theta(0, t) = \theta_0 \cos(\omega t) \tag{8}$$

In every layer, the heat diffusion equation for one-dimensional coordinate ( $x$ ) and time ( $t$ ) dependence without heat generation is received as:

$$\frac{\partial^2 \theta}{\partial x^2} = \frac{1}{\alpha} \frac{\partial \theta}{\partial t} \tag{9}$$

where  $\alpha$  is the thermal diffusivity and equal to  $k/\rho c_p$ ,  $k$  is the material thermal diffusivity,  $\rho$  is the material density and  $c_p$  is the material heat capacity. A trial will be done to solve the above equation by the variable's separation method. The temperature parameter as a function of two separated variables is written as:

$$\theta = \theta_x(x) \cdot \theta_t(t) \tag{10}$$

By placing the last connection into the above equation, it may be written as:

$$\theta_t(t) \cdot \frac{\partial^2 \theta_x(x)}{\partial x^2} = \frac{1}{\alpha} \cdot \theta_x(x) \cdot \frac{\partial \theta_t(t)}{\partial t} \tag{11}$$

After dividing the above equation by  $\theta_x(x) \cdot \theta_t(t)$ , it is received as:

$$\frac{1}{\theta_x(x)} \cdot \frac{\partial^2 \theta_x(x)}{\partial x^2} = \frac{1}{\alpha} \cdot \frac{1}{\theta_t(t)} \frac{\partial \theta_t(t)}{\partial t} \tag{12}$$

or as:

$$\alpha \cdot \frac{1}{\theta_x(x)} \cdot \frac{\partial^2 \theta_x(x)}{\partial x^2} = \frac{1}{\theta_t(t)} \frac{\partial \theta_t(t)}{\partial t} \tag{13}$$

Since the left side of the above equation is a function of  $x$  only and the right side is a function of  $t$  only, the two sides of the equation have to be equal to a constant. The following constant will be taken:

$$\alpha \cdot \frac{1}{\theta_x(x)} \cdot \frac{\partial^2 \theta_x(x)}{\partial x^2} = \frac{1}{\theta_t(t)} \frac{\partial \theta_t(t)}{\partial t} = i\omega \tag{14}$$

where  $i$  is the imaginary unit. It can be written that:

$$\frac{1}{\theta_t(t)} \frac{\partial \theta_t(t)}{\partial t} = i\omega \tag{15}$$

and that:

$$\frac{1}{\theta_t(t)} \frac{d\theta_t(t)}{dt} = i\omega \tag{16}$$

or as:

$$\frac{d\theta_t(t)}{\theta_t(t)} = i\omega dt \tag{17}$$

The solution of the time dependence part will be received by the continuing following steps:

$$\ln[\theta_t(t)] = i\omega t + C_1 \tag{18}$$

$$\theta_t(t) = e^{i\omega t + C_1} = C_1 e^{i\omega t} \tag{19}$$

The temperature location dependence will be received by developing the left side of the Eq. 13, continuing with the following steps:

$$\alpha \cdot \frac{1}{\theta_x(x)} \cdot \frac{d^2 \theta_x(x)}{dx^2} = i\omega \tag{20}$$

$$\frac{d^2 \theta_x(x)}{dx^2} - \frac{i\omega}{\alpha} \theta_x(x) = 0 \tag{21}$$

$$\left(D^2 - \frac{i\omega}{\alpha}\right) \theta_x(x) = 0 \rightarrow D_{1,2} = \pm \sqrt{\frac{i\omega}{\alpha}} \tag{22}$$

The full solution is received as:

$$\theta = \left[ C_2 \exp\left(\sqrt{\frac{i\omega}{\alpha}} x\right) + C_3 \exp\left(-\sqrt{\frac{i\omega}{\alpha}} x\right) \right] C_1 e^{i\omega t} \tag{23}$$

or as:

$$\theta = \left[ C_4 \exp\left(\sqrt{\frac{i\omega}{\alpha}} x\right) + C_5 \exp\left(-\sqrt{\frac{i\omega}{\alpha}} x\right) \right] e^{i\omega t} \tag{24}$$

where  $C_4 = C_1 \cdot C_2$  and  $C_5 = C_1 \cdot C_3$ .

Using the following connection:

$$\sqrt{i} = \frac{1}{\sqrt{2}} + i \frac{1}{\sqrt{2}} \tag{25}$$

The full solution is received as:

$$\theta = \left\{ C_4 \exp\left[\left(\sqrt{\frac{\omega}{2\alpha}} + i\sqrt{\frac{\omega}{2\alpha}}\right)x\right] + C_5 \exp\left[-\left(\sqrt{\frac{\omega}{2\alpha}} + i\sqrt{\frac{\omega}{2\alpha}}\right)x\right] \right\} e^{i\omega t} \tag{26}$$

The significance of the coefficients will now be changed according to the system structure:

$$\theta_1 = C_1 \exp\left\{\left[\left(\sqrt{\frac{\omega}{2\alpha_1}} + i\sqrt{\frac{\omega}{2\alpha_1}}\right)x\right] + i\omega t\right\} + C_2 \exp\left\{\left[-\left(\sqrt{\frac{\omega}{2\alpha_1}} + i\sqrt{\frac{\omega}{2\alpha_1}}\right)x\right] + i\omega t\right\} \tag{27}$$

$$\theta_2 = C_3 \exp\left\{\left[\left(\sqrt{\frac{\omega}{2\alpha_2}} + i\sqrt{\frac{\omega}{2\alpha_2}}\right)x\right] + i\omega t\right\} + C_4 \exp\left\{\left[-\left(\sqrt{\frac{\omega}{2\alpha_2}} + i\sqrt{\frac{\omega}{2\alpha_2}}\right)x\right] + i\omega t\right\} \tag{28}$$

where  $\theta_1$  is the relative temperature into the first layer and  $\theta_2$  is the relative temperature into the second layer.

The following boundary condition leads to knowing  $C_3$ :  
 $\theta_2|_{x \rightarrow \infty} = 0 \rightarrow C_3 = 0$  (29)

The following boundary condition leads to the next coefficients connection:

$$\theta_1|_{x=0} = \theta_0 \exp(i\omega t) \quad (30)$$

It is received that:

$$C_1 \exp(i\omega t) + C_2 \exp(i\omega t) = \theta_0 \exp(i\omega t) \quad (31)$$

Dividing the above connection by  $\exp(i\omega t)$  leads to the following coefficients connection:

$$C_1 + C_2 = \theta_0 \rightarrow C_2 = \theta_0 - C_1 \quad (32)$$

The third boundary condition leads to the following coefficients connection:

$$\theta_1|_{x=L} = \theta_2|_{x=L} \quad (33)$$

or to:

$$\begin{aligned} C_1 \exp\left\{\left[\left(\sqrt{\frac{\omega}{2\alpha_1}} + i\sqrt{\frac{\omega}{2\alpha_1}}\right)L\right] + i\omega t\right\} \\ + C_2 \exp\left\{\left[-\left(\sqrt{\frac{\omega}{2\alpha_1}} + i\sqrt{\frac{\omega}{2\alpha_1}}\right)L\right] + i\omega t\right\} = \\ = C_4 \exp\left\{\left[-\left(\sqrt{\frac{\omega}{2\alpha_2}} + i\sqrt{\frac{\omega}{2\alpha_2}}\right)L\right] + i\omega t\right\} \end{aligned} \quad (34)$$

Dividing by  $\exp(i\omega t)$  the following connection is received:

$$\begin{aligned} C_1 \exp\left[\left(\sqrt{\frac{\omega}{2\alpha_1}} + i\sqrt{\frac{\omega}{2\alpha_1}}\right)L\right] + C_2 \exp\left[-\left(\sqrt{\frac{\omega}{2\alpha_1}} + i\sqrt{\frac{\omega}{2\alpha_1}}\right)L\right] \\ = C_4 \exp\left[-\left(\sqrt{\frac{\omega}{2\alpha_2}} + i\sqrt{\frac{\omega}{2\alpha_2}}\right)L\right] \end{aligned} \quad (35)$$

The fourth boundary condition leads to the following coefficients connections:

$$k_1 \frac{\partial \theta_1}{\partial x} \Big|_{x=L} = k_2 \frac{\partial \theta_2}{\partial x} \Big|_{x=L} \quad (36)$$

$$\begin{aligned} k_1 \left\{ C_1 \left[ \left( \sqrt{\frac{\omega}{2\alpha_1}} + i\sqrt{\frac{\omega}{2\alpha_1}} \right) \exp\left\{ \left[ \left( \sqrt{\frac{\omega}{2\alpha_1}} + i\sqrt{\frac{\omega}{2\alpha_1}} \right) x \right] + i\omega t \right\} \right] + \right. \\ \left. + C_2 \left[ - \left( \sqrt{\frac{\omega}{2\alpha_1}} + i\sqrt{\frac{\omega}{2\alpha_1}} \right) \exp\left\{ \left[ - \left( \sqrt{\frac{\omega}{2\alpha_1}} + i\sqrt{\frac{\omega}{2\alpha_1}} \right) x \right] + i\omega t \right\} \right] \right\} \Big|_{x=L} \\ = k_2 C_4 \left[ - \left( \sqrt{\frac{\omega}{2\alpha_2}} + i\sqrt{\frac{\omega}{2\alpha_2}} \right) \exp\left\{ \left[ - \left( \sqrt{\frac{\omega}{2\alpha_2}} + i\sqrt{\frac{\omega}{2\alpha_2}} \right) x \right] + i\omega t \right\} \right] \Big|_{x=L} \end{aligned} \quad (37)$$

It is received that:

$$\begin{aligned} k_1 \left\{ C_1 \left[ \left( \sqrt{\frac{\omega}{2\alpha_1}} + i\sqrt{\frac{\omega}{2\alpha_1}} \right) \exp\left\{ \left[ \left( \sqrt{\frac{\omega}{2\alpha_1}} + i\sqrt{\frac{\omega}{2\alpha_1}} \right) L \right] + i\omega t \right\} \right] + \right. \\ \left. + C_2 \left[ - \left( \sqrt{\frac{\omega}{2\alpha_1}} + i\sqrt{\frac{\omega}{2\alpha_1}} \right) \exp\left\{ \left[ - \left( \sqrt{\frac{\omega}{2\alpha_1}} + i\sqrt{\frac{\omega}{2\alpha_1}} \right) L \right] + i\omega t \right\} \right] \right\} \\ = k_2 C_4 \left[ - \left( \sqrt{\frac{\omega}{2\alpha_2}} + i\sqrt{\frac{\omega}{2\alpha_2}} \right) \exp\left\{ \left[ - \left( \sqrt{\frac{\omega}{2\alpha_2}} + i\sqrt{\frac{\omega}{2\alpha_2}} \right) L \right] + i\omega t \right\} \right] \end{aligned} \quad (38)$$

The above equation can be divided by  $\exp(i\omega t)$  to get:

$$\begin{aligned} k_1 \left\{ C_1 \left[ \left( \sqrt{\frac{\omega}{2\alpha_1}} + i\sqrt{\frac{\omega}{2\alpha_1}} \right) \exp\left[ \left( \sqrt{\frac{\omega}{2\alpha_1}} + i\sqrt{\frac{\omega}{2\alpha_1}} \right) L \right] \right] + \right. \\ \left. + C_2 \left[ - \left( \sqrt{\frac{\omega}{2\alpha_1}} + i\sqrt{\frac{\omega}{2\alpha_1}} \right) \exp\left[ - \left( \sqrt{\frac{\omega}{2\alpha_1}} + i\sqrt{\frac{\omega}{2\alpha_1}} \right) L \right] \right] \right\} \\ = k_2 C_4 \left[ - \left( \sqrt{\frac{\omega}{2\alpha_2}} + i\sqrt{\frac{\omega}{2\alpha_2}} \right) \exp\left[ - \left( \sqrt{\frac{\omega}{2\alpha_2}} + i\sqrt{\frac{\omega}{2\alpha_2}} \right) L \right] \right] \end{aligned} \quad (39)$$

By marking:

$$a_1 = \sqrt{\frac{\omega}{2\alpha_1}} + i\sqrt{\frac{\omega}{2\alpha_1}} \quad (40)$$

and:

$$a_2 = \sqrt{\frac{\omega}{2\alpha_2}} + i\sqrt{\frac{\omega}{2\alpha_2}} \quad (41)$$

The third boundary condition leads to the following connection:

$$C_1 \exp(a_1 L) + C_2 \exp(-a_1 L) = C_4 \exp(-a_2 L) \quad (42)$$

and the fourth boundary condition leads to the following connections:

$$\begin{aligned} k_1 [C_1 a_1 \exp(a_1 L) + C_2 (-a_1) \exp(-a_1 L)] \\ = k_2 C_4 (-a_2) \exp(-a_2 L) \end{aligned} \quad (43)$$

$$\begin{aligned} C_1 k_1 a_1 \exp(a_1 L) - C_2 k_1 a_1 \exp(-a_1 L) \\ = -C_4 k_2 a_2 \exp(-a_2 L) \end{aligned} \quad (44)$$

Developing the third boundary condition will lead to following connections:

$$C_1 \exp(a_1 L) + (\theta_0 - C_1) \exp(-a_1 L) = C_4 \exp(-a_2 L) \quad (45)$$

$$\begin{aligned} C_1 [\exp(a_1 L) - \exp(-a_1 L)] + \theta_0 \exp(-a_1 L) \\ = C_4 \exp(-a_2 L) \end{aligned} \quad (46)$$

Dividing the above connection by  $\exp(-a_2 L)$  leads to the following connection:

$$\begin{aligned} C_4 = C_1 \{ \exp[(a_1 + a_2)L] - \exp[(-a_1 + a_2)L] \} \\ + \theta_0 \exp[(-a_1 + a_2)L] \end{aligned} \quad (47)$$

By marking:

$$a_3 = \exp[(a_1 + a_2)L] - \exp[(-a_1 + a_2)L] \quad (48)$$

$$a_4 = \theta_0 \exp[(-a_1 + a_2)L] \tag{49}$$

The following connection is received:

$$C_4 = a_3 C_1 + a_4 \tag{50}$$

By placing the values of  $C_2$  and  $C_4$  as a function of  $C_1$  into the fourth boundary condition, it leads to the following connections:

$$C_1 k_1 a_1 \exp(a_1 L) - (\theta_0 - C_1) k_1 a_1 \exp(-a_1 L) = (-a_3 C_1 - a_4) k_2 a_2 \exp(-a_2 L) \tag{51}$$

$$C_1 = \frac{\theta_0 k_1 a_1 \exp(-a_1 L) - a_4 k_2 a_2 \exp(-a_2 L)}{k_1 a_1 \exp(a_1 L) + k_1 a_1 \exp(-a_1 L) + a_3 k_2 a_2 \exp(-a_2 L)} \tag{52}$$

The exact temperature can be calculated by the following simple connection:

$$T = \text{real}(\theta) + T_i \tag{53}$$

### Results and Discussion

In all the following figures titles, the density  $\rho$  is designated as d, the specific heat  $c_p$  is designated as c, and the thermal diffusivity  $\alpha$  is designated as al, all with the lower index indicates belonging to layer 1 or 2.

Figures 2, 3 and 4 introduce a principally plots to show the effect of the thermal conductivities on the temperature distribution. The boundary layer between the two layers is at  $x = 1$ . The lines plot in the figure designates the relative temperature distribution every eighth period time. The frequency of the temperature oscillations was taken as  $\omega = 1$  and so the period time is equal to  $2\pi/\omega = 2\pi$ . Plot t1

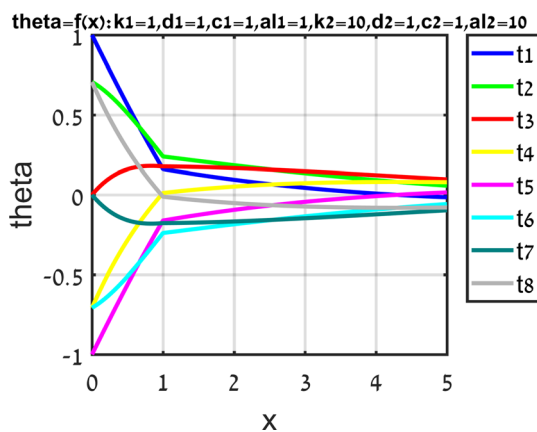


**Fig. 2** Relative temperatures distributions in accordance to the parameters listed in the figure title.  $t_1$  to  $t_8$  note the temperature distribution plots at time intervals of the eighth time period. Since the oscillations frequency was taken as  $\omega = 1$ , the time period is received as  $T = 2\pi/1 = 2\pi$ .  $t_1$  plot notes the temperature distribution at  $t = 0$  or at  $t = 2\pi$ .  $t_2$  plot notes the temperature distribution at  $t = 2\pi/8 = 0.7854$ .  $t_3$  plot notes the temperature distribution at  $t = 2 \times 2\pi/8 = 1.5708$  and so on.  $t_8$  plot notes the temperature distribution at  $t = 7 \times 2\pi/8 = 5.4978$

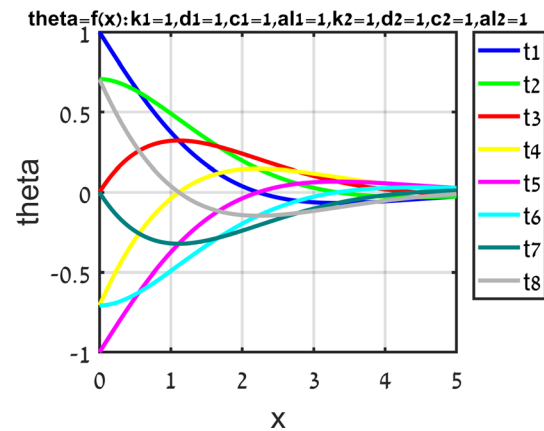


**Fig. 3** Relative temperatures distributions in accordance to the parameters listed in the figure title.  $t_1$  to  $t_8$  note the temperature distribution plots at time intervals of the eighth time period. Since the oscillations frequency was taken as  $\omega = 1$ , the time period is received as  $T = 2\pi/1 = 2\pi$ .  $t_1$  plot notes the temperature distribution at  $t = 0$  or at  $t = 2\pi$ .  $t_2$  plot notes the temperature distribution at  $t = 2\pi/8 = 0.7854$ .  $t_3$  plot notes the temperature distribution at  $t = 2 \times 2\pi/8 = 1.5708$  and so on.  $t_8$  plot notes the temperature distribution at  $t = 7 \times 2\pi/8 = 5.4978$

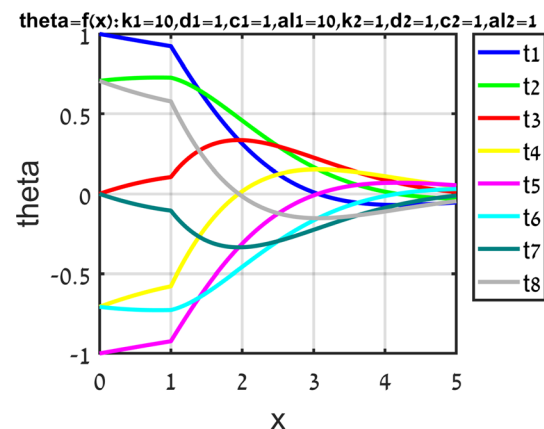


**Fig. 4** Relative temperatures distributions in accordance to the parameters listed in the figure title.  $t_1$  to  $t_8$  note the temperature distribution plots at time intervals of the eighth time period. Since the oscillations frequency was taken as  $\omega = 1$ , the time period is received as  $T = 2\pi/1 = 2\pi$ .  $t_1$  plot notes the temperature distribution at  $t = 0$  or at  $t = 2\pi$ .  $t_2$  plot notes the temperature distribution at  $t = 2\pi/8 = 0.7854$ .  $t_3$  plot notes the temperature distribution at  $t = 2 \times 2\pi/8 = 1.5708$  and so on.  $t_8$  plot notes the temperature distribution at  $t = 7 \times 2\pi/8 = 5.4978$

designates the relative temperature distribution at  $t = 0$  and plot t8, for example, designates the temperature distribution after seven eighth of the period time ( $7 \times 2\pi/8 = 5.4978$ ). Index 1 designates the physical parameters relate to layer 1 and index 2 designates the physical parameters relate to layer 2, ‘k’ ( $k$ ) is the thermal conductivity, ‘d’ ( $d$ ) is the material density, ‘c’ ( $c$ ) is the specific heat capacity, and ‘al’ ( $\alpha$ ) is the thermal diffusivity.

Figure 2 shows the effect of the increased thermal conductivity into the right slab on the relative temperature distribution. It is shown that at  $x = 5$  the maximum relative temperature is equal to 0.0968 and at  $x = 1$  the maximum relative temperature is equal to 0.2395.

Figure 3 shows the effect of the decreased conductivity or smaller equal thermal conductivities into the two layers on the relative temperature distribution. It is shown that at  $x = 5$  the maximum relative temperature is equal to 0.0269 and at  $x = 1$  the maximum relative temperature is equal to 0.4916.

By examining and comparing the two Figs. 2 and 3 and the above data, it is shown as was expected that the relative temperature oscillations in Fig. 2 where the second slab has the larger thermal conductivity restrained along the longer distance. But, it is noteworthy to be written and clearly was not expected that in the boundary between the two slabs, the figure with the reduced thermal conductivity shows larger oscillations. This result can be explained by energy conservation insight. On the left surface, the surface where  $x = 0$ , there are the same oscillations and amplitudes in the two structures represented by the two Figs. 2 and 3. The structure represented by Fig. 2 has an overall thermal resistance smaller than that represented Fig. 3 as a result of larger thermal conductivities along the two layers. So, it has to be concluded that the heat flux on the external surface of Fig. 2 structure at  $x = 0$  need to be larger than Fig. 3 structure and since that layer 1 of the two structures has identical values, the absolute gradient of Fig. 2 structure has to be larger than Fig. 3 structure. Also, according to an overall insight based on the larger conductivity of Fig. 2 structure in layer 2 and smaller overall thermal resistance, the temperature oscillations of Fig. 2 structure restrained along larger distance which can be clearly seen on the external left surfaces at  $x = 5$ , the maximum relative temperature value at Fig. 2 is larger than the maximum relative temperature value at Fig. 3.

Figure 4 introduce a principally plot to show the effect of the increased thermal conductivity into the left slab on the relative temperature distribution. It is shown that at  $x = 5$  the maximum relative temperature is equal to 0.0538 and at  $x = 1$  the maximum relative temperature is equal to 0.9234. The relative temperature gradient on the external surface at  $x = 0$  is smaller than the relative temperature gradients shown at Fig. 3. This can be explained as a result of the larger conductivity of layer 1 in Fig. 4, a large conductivity does not need a large temperature gradient to transfer the heat flux.

Along all the lines plot in Figs. 2, 3 and 4, it is shown that related to the two layers the temperature absolute value decreases along the depth coordinate ( $x$ ).

In Figs. 2 and 4, where there is a change in the thermal conductivity there is a change in the temperature gradient

at the separating surface at  $x = 1$ . When the thermal conductivity increases as in Fig. 2, the absolute value of the temperature gradient decreases. When the thermal conductivity decreases as in Fig. 4, the absolute value of the temperature gradient increases. This is of course due to the identity in the calculation of the heat flux along the separating surface based on layer 1 or based on layer 2,  $-k_1 \partial T_1 / \partial x|_{x=1} = -k_2 \partial T_2 / \partial x|_{x=1}$  or  $k_1 \partial T_1 / \partial x|_{x=1} = k_2 \partial T_2 / \partial x|_{x=1}$ . This physical condition leads to either temperature drop or to either a sharp rise in temperature.

It can be seen in Fig. 2, 3 and 4 that except in the constraint surface at  $x = 0$  where their value is zero and there are certain times when the temperatures are all either positive or either negative along all medium depth. These times are indicated by the plots t3 and t7. These are the times that indicate the temperature distribution after a quarter period time and after a three-quarter period time, respectively. This description is most clearly shown in Fig. 3 which represent an equal thermal conductivity in layer 1 and in layer 2. Plot t3 and plot t7 represent the last times before a negative or a positive trend change is imposed on the surface constraint at  $x = 1$ .

Plots t3 and t7 in Fig. 2, 3 and 4 show also acceptance of extreme temperature or extreme surfaces where the temperature is maximum or minimum. It is worth noting that these surfaces indicate the existence of adiabatic surfaces at these times. It can be noted that the heat enters along the medium depth until that adiabatic surfaces and does not pass on. On the other hand, heat exits from the area or volume defined by the constraint surface at  $x = 0$  to those adiabatic surfaces.

In Fig. 2, at times t1 and t5, it can be seen that the temperature distribution is linear along all the medium depth, both in the first and in the second layer. There are two factors that may contribute to this distribution kind. One factor is the lower thermal conductivity of the first layer which in fact is a resistance to heat transfer or to temperature change within the medium. The second factor relates to times t1 and t5, these times are the extremes of the temperature constraint because they indicate the start time period and the half time period. These times can be estimated as weakened times in terms of transient heat transfer and in fact strengthen the closeness to a steady heat transfer, plus the assumptions that exist here, no heat generation, one-dimensional heat transfer and constant thermal conductivity. All these may support the linear temperature distribution result. In Fig. 3, in which the thermal conductivity is uniform, there is no discontinuity in the thermal conductivity in both layers 1 and 2. In fact, one uniform layer is obtained. Here, there is no breaking in the temperature distribution and no temperature distribution of straight lines. Probably where possible, the temperature

distribution would be a natural continuity with no straight lines.

Figure 5 shows a real plot related to real parameters that was taken from a structural building materials list suited to a part of house wall composition. Layer 1 made of gypsum plaster was taken as the external layer exposed to the temperature environment. The gypsum plaster parameters are: material density  $\rho_1 = 1680 \text{ kg/m}^3$ , material thermal conductivity  $k_1 = 0.22 \text{ W/m} \cdot ^\circ \text{C}$  and specific heat capacity  $c_{p1} = 1085 \text{ J/kg} \cdot ^\circ \text{C}$ . Layer 2 which is the main building material of the wall was taken as common brick. The brick parameters are: material density  $\rho_2 = 1920 \text{ kg/m}^3$ , material thermal conductivity  $k_2 = 0.72 \text{ W/m} \cdot ^\circ \text{C}$  and specific heat capacity  $c_{p2} = 835 \text{ J/kg} \cdot ^\circ \text{C}$ . Layer 1 thickness was taken as 2 cm, and Layer 2 thickness was taken as 8 cm. The temperature amplitude between day and night was taken as  $\theta_0 = 10^\circ \text{C}$ . Twenty-four hours were taken for the period time and so the frequency is received as  $\omega = 2\pi/24_{\text{hours}} = 7.2722 \times 10^{-5} \text{ rad/s}$ . The parameters dimensions shown in the figure are:  $\theta [^\circ \text{C}]$ ,  $x [m]$ ,  $k [\text{kg/m} \cdot ^\circ \text{C}]$ ,  $d \equiv \rho [\text{kg/m}^3]$ ,  $c \equiv c_p [\text{J/kg} \cdot ^\circ \text{C}]$ ,  $al \equiv \alpha [\text{m}^2/\text{s}]$ . The figure shows the relative temperature oscillations along this part of the wall. The oscillations restraint after the plaster layer or at  $x = 2 \text{ cm}$  is received as  $5.4490^\circ \text{C}/10^\circ \text{C} = 0.5449 = 54.490\%$  and the oscillations restraint after the brick or at  $x = 10 \text{ cm}$  is received as  $2.6268^\circ \text{C}/10^\circ \text{C} = 0.26268 = 26.268\%$ . The brick restraint only is  $2.6268^\circ \text{C}/5.4490^\circ \text{C} = 0.4821 = 48.21\%$ . It should be noted that, in addition to the fact that the wall

prevents heat transfer to a cold environment, it also acts as a retainer for the temperature fluctuations or at an equal inference to the heat transfer oscillations.

A comparison of the amplitude absolute value between Figs. 5 and 2, 3, 4 indicates something about the validation of the physical model. It can be seen that the values of the temperatures along all the medium relative to the amplitude value decrease with decreasing the amplitude value. Another small move to validate the model was made by selecting a constant forced temperature by setting a zero value for amplitude. The temperature values obtained along the entire medium were zero as expected. There was no point in presenting this plot result.

### Summary

The physical model presented in this work for a finite material thickness inserted within the semi-infinite medium can be applied for an additional number of material layers. It was shown that the structure with the overall smaller thermal resistance due to a larger conductivity in the semi-infinite medium leads to a larger absolute gradient of temperature value at the external surface at  $x = 0$ . At the times after a quarter period time and after a three-quarter period time, temperature distributions with extreme, maximum or minimum temperatures values are received. These values actually represent adiabatic surfaces at these times, meaning that heat transfer, entry or exit occurs in the limited volume between the constraint surface and those adiabatic surfaces. These temperature distributions also show receiving of identical, positive or negative values along all the medium depth. At the start time of the time period and at the half time of the time period, linear temperatures distributions are obtained. These times can be seen as weakening times in terms of supporting the transient heat transfer. The temperature distribution in the structure of a wall made up of real building materials shows that the wall is a retainer for temperature fluctuations and not just is a basic resistance to heat transfer. Using complex numbers are a very efficient tool for analysing such research directions. Linear physical models have very high capacity of describing most important physical phenomena.

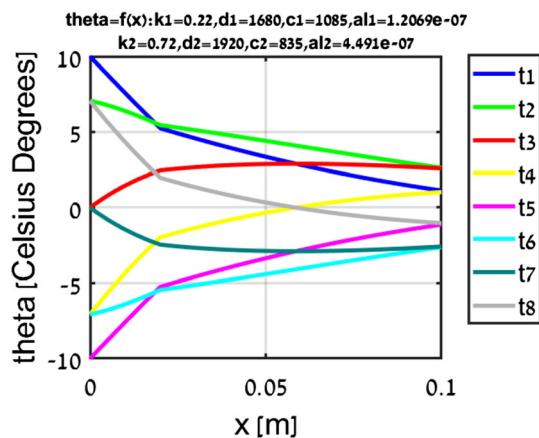


**Fig. 5** Relative temperature distributions along a real wall (the relevant parameters are listed in the figure title).  $t_1$  to  $t_8$  note the temperature distribution plots at time intervals of the eighth time period. The time period was taken as  $T = 24 \text{ hours} = 86,400 \text{ seconds}$  (-).  $t_1$  plot notes the temperature distribution at  $t = 0$  or at  $t = 24 \text{ hours} = 86,400 \text{ seconds}$ .  $t_2$  plot notes the temperature distribution at  $t = 24/8 = 3 \text{ hours} = 10,800 \text{ seconds}$ .  $t_3$  plot notes the temperature distribution at  $t = 2 \times 24/8 = 6 \text{ hours} = 21,600 \text{ seconds}$  and so on.  $t_8$  plot notes the temperature distribution at  $t = 7 \times 24/8 = 21 \text{ hours} = 75,600 \text{ seconds}$

### References

1. H. Schlichting, *Boundary Layer Theory* (McGraw Hill, New York, 1979).
2. R. Panton, The transient for Stokes's oscillating plate: a solution in terms of tabulated functions. *J. Fluid. Mech.* **31**(4), 819–825 (1968)

3. M. Nazar, C.O. Fetecau, D. Vieru, C. Fetecau, New exact solution corresponding to the second problem of Stokes for second grade fluids. *Nonlinear. Anal. Real. World. Appl.* **11**, 584–591 (2010)
4. S. Asghar, S. Nadeem, K. Hanif, T. Hayat, Analytic solution of Stokes second problem for second-grade fluid, Hindawi Publishing Corporation. *Math. Probl. Eng.* **72468**, 1–8 (2006)
5. S. Srinivasan, K.R. Rajagopal, Study of a variant Stokes' first and second problems for fluids with pressure dependent viscosities. *Int. J. Eng. Sci.* **47**, 1357–1366 (2009)
6. V. Prusa, Revisiting Stokes first and second problems for fluids with pressure dependent viscosities. *Int. J. Eng. Sci.* **48**, 2054–2065 (2010)
7. P. Datta, A. Beskok, Analytical solution of time periodic electroosmotic flows: analogies to stokes' second problem. *Anal. Chem.* **73**, 5097–5102 (2001)
8. A.-R.A. Khaled, Conduction heat and entropy transfer in a semi-infinite medium and wall with a combined periodic heat flux and convective boundary condition. *Int J Therm Sci* **47**, 76–83 (2008)
9. H. Ahmadikia, R. Fazali, A. Moradi, Analytical solution of the parabolic and hyperbolic heat transfer equations with constant and transient heat flux conditions on skin tissues. *Int Commun Heat Mass Transf* **39**, 121–130 (2012)
10. H. Sadat, A second order model for transient heat conduction in a slab with convective boundary conditions. *Appl Therm Eng* **26**, 962–965 (2006)
11. M. Norouzi, A.A. Delouei, M. Seilsepour, A general exact solution for heat conduction in multilayer spherical composite laminates. *Compos Struct* **106**, 288–295 (2013)
12. Y.C. Shiah, Y.X. Shi, Heat conduction across thermal barrier coatings of anisotropic substrates. *Int Commun Heat Mass Transf* **33**, 827–835 (2006)
13. B. Kundu, Exact analysis for propagation of heat in biological tissue subject to different surface conditions for therapeutic applications. *Appl Math Comput* **285**, 204–215 (2016)
14. B. Kundu, K.S. Lee, Thermal design of an orthotropic flat fin in fin-and-tube heat exchangers operating in dry and wet environments. *Int Heat Mass Transf* **54**, 5207–5214 (2011)
15. B. Kundu, K.S. Lee, An appropriate analysis for optimum design of wet fins based on modified 1-D and 2-D approaches. *Energy Convers Manag* **103**, 814–826 (2015)
16. G. Stokes, On the effect of the internal friction of fluids on the motion of pendulums. *Camb Philos Soc.* 9, 8–106 (1850). Reprinted in *mathematical and physical papers, Sir George Gabriel Stokes and Sir Larmor* **3**, 1880–1905

**Publisher's Note** Springer Nature remains neutral with regard to jurisdictional claims in published maps and institutional affiliations.